ACS APPLIED MATERIALS & INTERFACES

Research Article

www.acsami.org

Enhancement of the Stability of Fluorine Atoms on Defective Graphene and at Graphene/Fluorographene Interface

Zhimin Ao,*[,†] Quanguo Jiang,[‡] Shuang Li,[§] Hao Liu,[†] Francois M. Peeters,[∥] Sean Li,[⊥] and Guoxiu Wang*[,†]

[†]Centre for Clean Energy Technology, School of Mathematical and Physical Sciences, University of Technology Sydney, P.O. Box 123, Broadway, Sydney, New South Wales 2007, Australia

[‡]College of Mechanics and Materials, Hohai University, Nanjing 210098, China

[§]Nano Structural Materials Center, Nanjing University of Science and Technology, Nanjing 210094, Jiangsu P.R. China

[∥]Department of Physics, University of Antwerp, Groenenborgerlaan 171, B-2020 Antwerpen, Belgium

[⊥]School of Materials Science and Engineering, The University of New South Wales, Sydney, New South Wales 2052, Australia

ABSTRACT: Fluorinated graphene is one of the most important derivatives of graphene and has been found to have great potential in optoelectronic and photonic nanodevices. However, the stability of F atoms on fluorinated graphene under different conditions, which is essential to maintain the desired properties of fluorinated graphene, is still unclear. In this work, we investigate the diffusion of F atoms on pristine graphene, graphene with defects, and at graphene/fluorographene interfaces by using density functional theory calculations. We find that an isolated F atom diffuses easily on graphene, but those F atoms can be localized by inducing vacancies or absorbates in graphene and by creating graphene/fluorographene interfaces, which would strengthen the binding energy of F atoms on graphene and increase the diffusion energy barrier of F atoms remarkably.

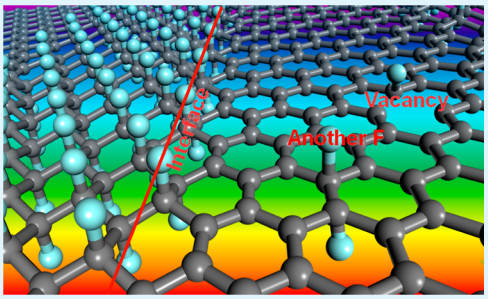

KEYWORDS: *graphene, density functional theory, thermal stability, fluorination, diffusion*

1. INTRODUCTION

In the past few years, covalently modified graphene derivatives prepared by attachment of hydrogen, halogens, or other atoms have attracted considerable interest to tune the properties of graphene for their potential applications,[1] such as in nanoelectronic devices and as hydrogen storage materials. Besides graphene oxide and graphane, fluorographene—fully fluorinated graphene—is another important structural derivative of graphene.[1−3] Fluorographene has a similar geometric structure to the sp^3 bonding configuration in graphane, with each carbon covalently bonded to one fluorine atom. Fluorinated graphene is synthesized mainly by reacting graphene with XeF_2 and F_2[4,5] or with CHF_3 and CF_4 plasma,[6,7] or by mechanical and chemical exfoliation of graphite fluoride.[8,9] The attachment of fluorine atoms to sp^2 carbons would significantly affect the electronic properties and the local structure of the material but preserves the 2D hexagonal symmetry. Such structural change would open the zero band gap of pristine graphene to ∼3 eV.[10] Fluorographene is also found to have high transparency and fascinating insulating properties, which makes it the world's thinnest transparent insulator, and it has great potential for future optoelectronic and photonic nanodevices.[11,12]

First-principles studies on graphene monofluoride started in 1993,[13] motivated by available experiments on graphite monofluoride. Theoretical calculations also predicted that partial fluorination of graphene from $C_{32}F$ to C_4F is able to increase the band gap from 0.8 to 2.9 eV.[2,14,15] As a result, through spatial selective fluorination of a graphene sheet using treatment by a low-damage CF_4 plasma, it should be possible to achieve conductive (pristine graphene), semiconductive (partially fluorinated graphene), and insulator (highly fluorinated graphene) areas in the same graphene sheet.[6] Moreover, fluorination of selective areas of graphene can also been achieved by removing F atoms from fluorographene by an electron beam[16] or by local deposition of F atoms through laser irradiation with fluoropolymers.[17] In addition, a recently experimentally realized lateral graphene/fluorographene hybrid nanoribbon field-effect transistor was found to exhibit a very high ON−OFF switching ratio of 10^5 at room temperature. These devices also demonstrated excellent current−voltage saturation, providing a potential path for active radio frequency application.[18] Such hybrid graphene/fluorographene nanoribbons have also been studied by first-principles calculations in order to investigate their structural and electronic properties.[10] It was found that the electronic and magnetic properties of hybrid graphene/fluorographene nanoribbons are tunable depending on the interface type (armchair or zigzag interface), the width of the nanoribbons and the termination of the edges,

Received: May 19, 2015
Accepted: August 24, 2015
Published: August 24, 2015

DOI: 10.1021/acsami.5b04319
ACS Appl. Mater. Interfaces 2015, 7, 19659−19665

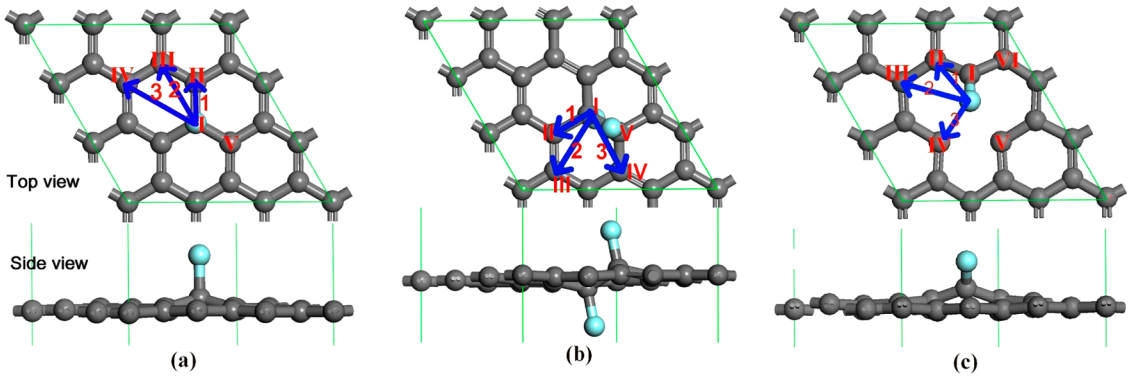

Figure 1. Supercell of graphene used in the calculations. (a) One F atom on pristine graphene, (b) two F atoms on pristine graphene, and (c) one F atom on graphene with a vacancy. In this and the following figures, the arrows indicate the different diffusion pathways considered. The gray and blue balls are C and F atoms, respectively.

which are promising for the realization of graphene-materials-based spintronics applications.

Although graphene fluoride and graphene/fluorographene hybrid nanoribbons have been found to have great potential for applications in optoelectronic and photonic nanodevices, the thermodynamic stability of F atoms on fluorinated graphene or at the graphene/fluorographene interface is not clearly understood, which is essential to maintain the excellent properties of graphene fluoride and graphene/fluorographene heterostructures. It is known from ab initio calculations[19,20] that the stability of H atoms at the interface of graphene/graphane nanoribbons can be enhanced significantly as compared with an isolated H atom on pristine, and it was predicted that graphene/graphane nanoribbons are stable down to the limit of a single carbon chain.[19] Therefore, it is expected that the stability of F atoms at the interface of graphene/fluorographene nanoribbons (GFNRs) would also be enhanced remarkably. In this work, the thermodynamic stability of F atoms on graphene and at the interface of GFNRs is studied using density functional theory (DFT) calculations through investigating the diffusion of F atoms on graphene and at the interface of GFNRs. Due to the presence of unavoidable defects in real graphene samples, the effects of defects, such as adsorbates and vacancies, on the stability of F atoms on graphene are also investigated. Stability enhancement mechanisms for F atoms on graphene are analyzed from the calculation of the binding energy and the electron transfer between F atoms and graphene.

2. CALCULATION DETAILS

The spin-polarized DFT calculations were executed using the DMOL^3 code. The generalized gradient approximation (GGA) with RPBE functional was utilized as the exchange−correlation functional. A double numerical plus polarization (DNP) was used as the basis set, while the DFT semicore pseudopotentials (DSPP) core treatment was utilized to include relativistic effects. Spin polarization was included in the calculations. The convergence tolerance of the energy was set to 10^{-5} Ha (1 Ha = 27.21 eV), and the maximum allowed force and displacement were 0.02 Ha and 0.005 Å, respectively. To inspect the diffusion pathways of fluorine atoms at the graphene surface, linear synchronous transition/quadratic synchronous transition (LST/QST) and nudged elastic band (NEB) tools in the DMOL^3 code were employed. The k-point is set as 12 × 12 × 1 to search for the structure of the transition state (TS) and the minimum energy pathway. In the simulations, 18 Å vacuum over the graphene layer is taken to minimize the interlayer interactions, three-dimensional periodic boundary conditions were imposed, and all the atoms are allowed to relax. The DFT-D method within the Grimme scheme is used in all calculations to consider the van der Waals forces.[21] The binding energy (E_b) of a F−C bond was determined by

$$E_b = E_i - (E_{i-F} + E_F) \quad (1)$$

where E_i is the total energy of the initial system, E_{i-F} is the total energy of the initial system after removing one F atom, and E_F is the energy of an isolated F atom.

3. RESULTS AND DISCUSSION

3.1. Stability of a Single F Atom on Pristine Graphene.

Previously the stability of fluorinated graphene with different degree of fluorination was mainly determined from the binding energy and the length of the F−C bonds, and the electron transfer between F and C atoms.[3,22−24] However, the mobility of F atoms on fluorinated graphene was not investigated, which, however, is an important property relevant for different applications. This motivated us to focus on the investigation of the mobility of F atoms on fluorinated graphene and to propose different methods to tune the diffusion energy barriers. First the diffusion of an isolated F atom on graphene will be investigated. Figure 1a shows the used supercell of graphene in our calculation. An F atom is chemically adsorbed on the C atom at position I as indicated in Figure 1a. For the F atom, there are three different possible diffusion pathways as shown in Figure 1a: to the nearest C (path 1), to the second nearest position (path 2), and to the opposite position (path 3). The relaxed atomic structure with one F atom adsorbed on graphene is shown in Figure 1a, where we see that the F atom induces a local structural deformation of the graphene lattice. The C atom bounded to the F atom protrudes from the graphene plane due to the change of the bonding character from sp^2 to sp^3-like hybridization, similar to the case of hydrogenated graphene.[25] This also agrees with previous reported result.[26] The obtained binding energy of the F−C bond E_b is −1.92 eV with bond length l_{F-C} = 1.535 Å. Previous reports showed that E_b and l_{F-C} exhibit a strong dependence on the degree of graphene fluorination,[15,22] where E_b varied from −1.48 to −3.41 eV with corresponding l_{F-C} from 1.383 to 1.572 Å. In this work, as shown in Figure 1 the degree of fluorination is 1 F atom per 18 C atoms. The obtained E_b and

DOI: 10.1021/acsami.5b04319
ACS Appl. Mater. Interfaces 2015, 7, 19659−19665

l_{F-C} are consistent with the reported results of −2.32 eV and 1.565 Å,[15] ∼ 2.0 eV and ∼1.6 Å[22] for a similar degree of fluorination. It is known that the chemical adsorption of F atoms alters the electronic and magnetic properties of graphene and opens up a bandgap.[26,28] The electronic and magnetic properties of fluorinated graphene have been discussed in previous work. Here we will focus on the thermodynamic stability of F atoms on graphene and at the graphene/fluorographene interface. Using LST/QST and NEB methods, all the three possible diffusion pathways of a F atom on pristine graphene as shown in Figure 1a are calculated, and the results are shown in Table 1, where the diffusion barrier E_{bar} is the energy difference between the energy of the transition state (TS) and of the initial structure (IS) before diffusion, and the diffusion energy E_R is the energy difference between the energy of the final structure (FS) after diffusion and the initial structure (IS) before diffusion. To better understand the determination of the diffusion energy barrier and diffusion energy, the detailed diffusion pathway of an isolated F atom on graphene along path 1 is taken as an example and shown in Figure 2 where the atomic structures of IS, TS, and FS are also given as inserts. As shown in Figure 2, along the diffusion pathway there is a high-energy state-TS, which has an energy of 0.41 eV higher than that of IS (i.e., the diffusion energy barrier is 0.41 eV). As one can see, at TS the F atom desorbs from graphene and locates at the bridge site of the C−C bond. From the results listed in Table 1, it is found that the diffusion barrier for the two possible pathways 1 and 2 are very close to ∼0.40 eV. The corresponding barrier for pathway 3 is 0.54 eV, which is much higher owing to the longer diffusion distance and the fact that more C atoms are involved in the diffusion. Note that there is no energy difference between the states before and after diffusion for all three diffusion pathways. This is understandable because all the C atoms have the same potential energy. Therefore, the lowest energy barrier for an isolated F atom on graphene is ∼0.40 eV, which compares with the reported value of 0.36 eV for the diffusion of a single F atom on a 2 × 2 graphene supercell (i.e., which corresponds to a much higher F-concentration).[22] In general it is considered that a surface reaction at ambient temperature occurs when the energy barrier is smaller than 0.91 eV.[27] In addition, the diffusion time at room temperature is given by Arrhenius equation[29]

$$\tau = \frac{1}{\nu e^{(-E_{bar}/k_B T)}} \quad (2)$$

where ν is of the order of 10^{12} Hz, k_B is the Boltzmann constant, and T = 298.15 K. For diffusion of an F atom on graphene we find $\tau = 5.78 \times 10^{-6}$ s. Therefore, at room temperature a single F atom has a rather high mobility on the graphene surface. To further demonstrate its mobility, the diffusion coefficient D of a single F atom on pristine graphene is determined by the equation,[30] $D = Pd^2\nu \exp(-E_{bar}/k_B T)$, where $P = 1/3$ comes from the nearest probable positions for the F atom to jump, $d \sim 1.42$ Å is the jump distance that is equal to the C−C bond length, E_{bar} is the calculated diffusion barrier of 0.40 eV, the temperature is 300 K, and the vibration frequency ν of a C atom is about 10^{12} Hz. A high diffusion coefficient 1.30×10^{-9} cm^2S^{-1} is obtained, which is comparable to the self-diffusion coefficient of liquid water.[31]

Table 1. Diffusion Barriers ($E_{TS} - E_{IS}$) for Several Diffusion Paths (See Figures 1 and 3) and Diffusion Energy ($E_{FS} - E_{IS}$) for F Atom Diffusing in the Presence of Different Environments

	diffusion pathways	diffusion energy (eV)	diffusion barrier (eV)
one F atom on graphene	1	0	0.41
	2	0	0.40
	3	0	0.54
two F atoms on graphene	1[a]		
	2	0.54	1.60
	3	−0.003	0.92
one F atom on graphene with vacancy	1	2.85	3.11
	2	1.80	2.88
	3	0	1.67
zigzag GFNR interface	1	1.27	1.92
	2	1.27	2.10
	3	1.01	2.40
	4	1.47	2.70
	5	1.50	2.68
armchair GFNR interface	6	1.28	2.26
	7	2.00	2.28
	8	1.14	2.28
	9	2.09	2.26
	10	2.34	2.27

[a]Diffusion could not happen. The F atom at site II will diffuse back to site I in Figure 1b automatically during the geometry optimization.

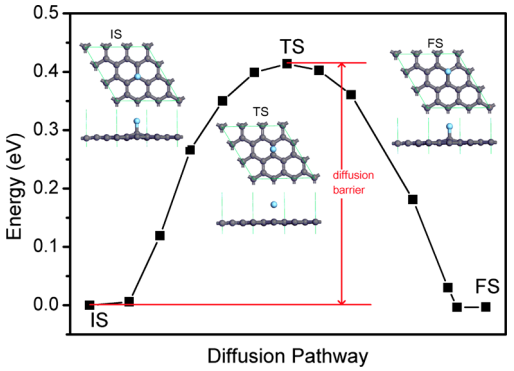

Figure 2. Diffusion pathway of an isolated F atom on pristine graphene along path 1. The diffusion energy barrier is the energy difference between TS and IS, whereas the diffusion energy is the energy difference between FS and IS. The energy of IS is set to be 0.

3.2. Stability of a Single F Atom on Defective Graphene. Some defects, such as vacancies, are unavoidable in graphene. The diffusion of a single F atom will be influenced by the presence of such nearby defects due to local changes of the electron distribution near the defect. Previous reports on the diffusion barrier of transition metal (TM) atoms on graphene found a substantial increase from 0.2 to 0.8 eV to 2.1−3.1 eV if the TM atoms are coupled to a vacancy.[32] Furthermore, it was found that the desorption of H atoms on N-doped graphene becomes much easier if there is another H atom nearby.[33] Therefore, we investigate the diffusion behavior of a F atom on graphene with another F atom or a vacancy nearby. If the first F atom is adsorbed at position IV in Figure 1b, the second F atom has four possible adsorption sites in the same carbon ring (i.e., positions I, II, III, and IV, near the first F atom). All the four possible configurations are calculated, and we find that the configuration with the second F atom adsorbed at position I has the lowest energy, which therefore is the favorite configuration for the two F atoms adsorbed on

DOI: 10.1021/acsami.5b04319
ACS Appl. Mater. Interfaces 2015, 7, 19659−19665

graphene. The corresponding structure is shown in Figure 1b. Similar to the previous case of a single F atom adsorbed on graphene, the two C atoms bounded with the two F atoms will protrude from the graphene layer. The binding energy of the F−C bond is −2.75 eV and the bond length is 1.484 Å which compares with E_b = −1.92 eV and l_{F-C}= 1.535 Å for the case of an isolated F atom. Thus, the binding is much stronger with shorter bond length. This also agrees with previous reports that E_b increases with increasing degree of fluorination.[22]

To consider the effect of another F atom bound to graphene on the diffusion behavior of F, we investigate the diffusion of the second F atom from position I to positions II, III, or IV when the other F atom is localized on the other side of graphene at position V. The three diffusion paths are indicated as paths 1, 2, and 3 in Figure 1b. The calculated results are listed in Table 1. It is found that pathway 1 could not happen. The F atom at site II would diffuse back to site I atomically when doing geometry optimization. Pathway 3 is preferred with the lowest diffusion energy barrier and negative diffusion energy. The low energy barrier for pathway 3 can be understood through an analysis of the atomic charges of the atoms at the five positions I−V. Based on Hirshfeld method,[34] it is known that the charges on the five C atoms at positions I−V are 0.09, −0.001, 0.013, 0.001, 0.091 *e*, respectively, whereas the charges on the two F atoms are the same −0.153 *e*. For the F diffusion along path 1, the attractive interaction is present between the negatively charged F atom and positively charged C atom at site I, although repulsive interaction is present between the negatively charged F atom and the negatively charged C atom at site II. This attractive to repulsive interaction transition prevents the occurrence of the diffusion pathway 1.

For the F diffusion along path 2, the diffusion is from site I to site III directly. This diffusion is still affected by the repulsive interaction between the F atom and the C atom at site II, which increases the diffusion barrier of this pathway. Although for the diffusion path 3, based on the TS search calculation, it is known that this diffusion is from site I to site V, then to site IV. The relatively strong attractive interaction between the F atom and the C atom at site V facilitates this diffusion, at the meantime the other F atom binding with the C atom at site V prevents the binding of another F atom with the same C atom. Therefore, the F atom would continue the diffusion to the site IV, and it is understandable that path 3 has the lowest diffusion barrier 0.92 eV. But it is still much higher than that of 0.40 eV for an isolated F atom diffusion on graphene, because the presence of another F atom nearby would change the electronic distribution and strengthen the F−C bonds, thus enhancing the stability of the F atoms on graphene.

Figure 1c shows the relaxed structure of one F atom chemically adsorbed on graphene with a vacancy. We find that the F atom prefers to adsorb at the C atoms at the vacancy, and its total energy is much lower than those of the other configurations after considering all the possible adsorption configurations. The F atom is found to be close to the center of the vacancy, and the F−C bond tilts to the graphene surface in contrast to F adsorbed on graphene without a vacancy. This is induced by the attractive interaction between the other two C atoms at the vacancy and the F atom. The binding energy of the F−C bond is −4.42 eV with a bond length of 1.350 Å. The obtained binding energy is much larger than −1.92 eV of the F−C bond on graphene without vacancy, and a shorter bond length is found in the vacancy system, which is similar to the case of TM atoms coupled with a vacancy in graphene.[32] To better understand the interactions of the F atom with the three C atoms at the vacancy, the atomic charge of the system is calculated through the Hirshfeld method.[34] The results show that the two C atoms at positions IV and V have the same positive charge of 0.0025 *e* due to the symmetry of the two atoms, and the charges of the F atom and the C atom at position I are −0.0686 and 0.0989 *e*, respectively. The two C atoms at positions II and VI have a net charge of −0.0098 *e*. Therefore, repulsive forces are present between the negatively charged F atom and the two C atoms at positions II and VI, whereas the F atom feels an attractive interaction with the two positively charged C atoms at positions IV and V. Given these electrostatic interactions, it is understandable that the F atom prefers to localize at nearly the center of the vacancy.

To understand the effect of the vacancy on the diffusion of the F atom on graphene, three possible diffusion pathways are calculated, as shown in Figure 1c, and the results are listed in Table 1. It shows that the diffusion barriers are substantially increased for all the three pathways as compared to the case of graphene without a vacancy. It is also found that the F atom prefers to diffuse among the three C atoms at the vacancy with a lower energy barrier of 1.67 eV, and there is no energy difference before and after diffusion. For the diffusion to positions II and III, much higher energy barriers of 3.11 and 2.88 eV are obtained, respectively. Therefore, vacancies can significantly enhance the thermodynamic stability of the F atom on graphene, and can be considered to be active sites and anchors for adsorbates. Note that, different from other cases, the attractive interactions between the two C atoms at positions IV and V and the F atom also contributes to the binding energy of the C−F bond when determined through eq 1 in the method section below. Therefore, the diffusion barrier among the three C atoms at the vacancy is relatively low due to the fact that only part of the C−F interaction needs to be broken for this type of diffusion.

3.3. Stability of F Atoms at the Graphene/Fluorographene Interface. It is known from the above discussion that the diffusion behavior of a single F atom is different if there is another F atom in its neighborhood. Therefore, it is expected that the diffusion behavior of an F atom at the interface of graphene/fluorographene nanoribbons will be remarkably modified due to the presence of F atoms at the graphene/fluorographene interface. As shown in Figure 3, there are two types of interfaces: zigzag (Figure 3a) and armchair (Figure 3b). For both types of nanoribbons, the C atoms protrude from the C layer due to the bonded F atoms, which changes the C atoms into sp^3-like binding. In addition, for the zigzag GFNRs, both the graphene and fluorographene nanoribbons are flat (see Figure 3a). However, the graphene and fluorographene layers are not in the same plane, and there is a tilt angle of about 150° at the interface, which is consistent with previous reported result.[10] For the armchair GFNRs (Figure 3b), the graphene and fluorographene regions are flat and in the same plane, which also agrees with ref 10. The interfaces between graphene and fluorographene nanoribbons are the interfaces between sp^2- and sp^3-bonded C atoms. C atoms in graphene have sp^2 hybridization and the structure stabilizes as a flat sheet. The hybridization changes from sp^2 to sp^3 in fluorographene due to the presence of alternating F atoms placed on both sides of the carbon plane. The sp^3 hybridization also forces nearest neighbor C atoms in fluorographene to lie in different planes. As shown in Figure 3a, the closed C atoms in fluorographene at the right side of the zigzag interface are only bonded with F

DOI: 10.1021/acsami.5b04319
ACS Appl. Mater. Interfaces 2015, 7, 19659−19665

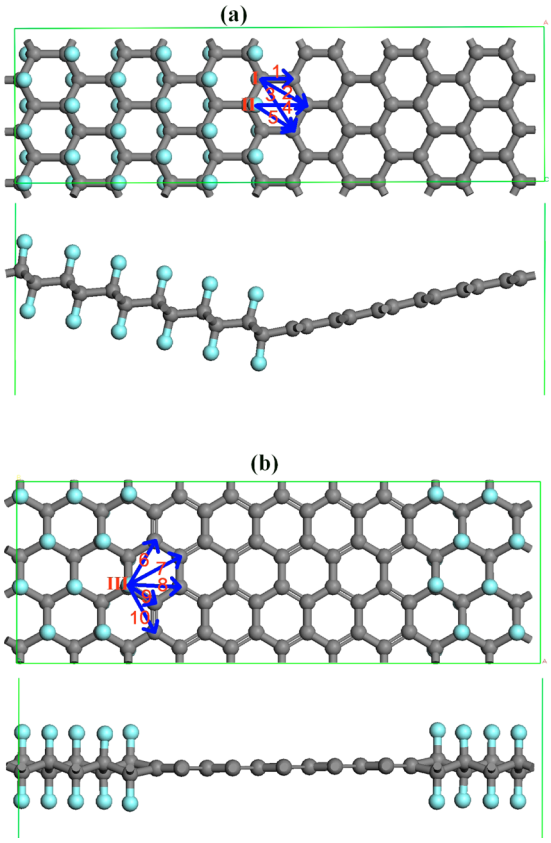

Figure 3. Atomic structure of graphene/fluorographene nanoribbons. (a) Zigzag and (b) armchair interfaces after geometry relaxation.

atoms below the fluorographene layer, which will push down the graphene nanoribbon due to the sp^3 hybridized C atoms. At the left side interface, the closed C atoms in fluorographene are only bonded with F atoms above the fluorographene layer, which would push up the graphene nanoribbon due to the sp^3 hybridized C atoms. This induces a tilt angle of ∼150° at the zigzag interface. For the armchair interface, the closed C atoms at both sides of the interface bind with the F atoms alternatingly above and below the fluorographene layer, as shown in Figure 3b. The pushing down and up forces at the interface are neutralized. Thus, the armchair graphene/fluorographene nanoribbons are flat without a tilt angle.

The stability of the two types of interfaces are analyzed by calculating the diffusion barriers of the F atoms at the interface. For the case of a zigzag interface, there are two different types of C and F atoms, which are indicated as sites I and II in Figure 3a. For the diffusion of the F atom at site I, there are three possible diffusion paths labeled as 1−3. For the F atom at site II, there are two possible diffusion pathways that we label as 4 and 5. In the case of an armchair interface, all the C atoms at the interface are equivalent from a diffusion point of view, and there are five different diffusion pathways that we label as 6−10 in Figure 3b. The diffusion barriers and diffusion energies for the different paths and for both types of graphene/fluorographene interfaces are summarized in Table 1. For the zigzag interface, it is found that the barriers are 1.92, 2.10, 2.40, 2.70, 2.68 eV for the pathways 1−5, respectively. Thus, the minimum diffusion barrier for the zigzag GFNRs is the F atom at site I diffusing to its nearest C atom along the C−C bond with an energy barrier of 1.92 eV. For the armchair interface, the energy barriers for pathways 6−10 are 2.26, 2.28, 2.28, 2.26, and 2.27 eV, respectively. Thus, the energy barrier for F diffusing at the armchair interface can be minimized to 2.26 eV to the second nearest C atom along path 6. For both zigzag and armchair interfaces, the minimum diffusion barriers of the F atoms are about 5 times larger than that of F diffusing on pristine graphene. In addition, the energy barriers for the F atom diffusing along the different paths at the armchair interface are almost the same ∼2.26 eV, which is larger than the minimum diffusion barrier of the F atoms at the zigzag interface. From Table 1, we notice that all the F diffusion processes at the interfaces imply an increase of a few eV of the energy of the system after diffusion, which indicates that after the diffusion the energy needed for recovering back to the initial perfect thermodynamic state is always lower than the energy needed for distorting the interfaces. Therefore, we can conclude that the graphene/fluorographene interfaces are stable at room temperature for both types of hybrid nanoribbon interfaces.

The stability enhancement can be understood by calculating the binding energy of the F atoms in the different situations, which are proportional to the strength of the C−F bonds. Previously it was found that the diffusion barrier for an isolated H atom on graphene is ∼0.3 eV, which was obtained by a DFT calculation using a similar method as in this work.[35] The higher diffusion barrier here for an isolated F atom on graphene is due to the stronger binding energy of the C−F bond (−1.92 eV) as compared to C−H (−0.88 eV).[20] For the F atoms in other systems, E_b in graphene with a vacancy is enhanced to −4.42 eV with l_{C-F} = 1.350 Å, and the E_b for the two F atoms on graphene is −2.73 eV with l_{C-F} = 1.484 Å. For the F atoms at the GFNRs interfaces, the binding energy of the C−F bond at sites I and II at the zigzag interface are −3.39 and −3.85 eV, respectively. The corresponding bond lengths are 1.400 and 1.395 Å. For the armchair interface of GFNRs, the bind energy at site III is −3.05 eV with a bond length of 1.405 Å. This indicates a stability enhancement of the F atoms on defected graphene and at the graphene/fluorographene interface due to the presence of stronger C−F bonds. The results for the binding energy and bond length also explain the increased stability: F at the vacancy (E_b = −4.42 eV, l_{C-F} = 1.350 Å) > F at site II of zigzag interface (E_b = −3.85 eV, l_{C-F} = 1.395 Å) > F at site I of zigzag interface (E_b = −3.39 eV, l_{C-F} = 1.400 Å) > F at site III of armchair interface (E_b = −3.05, l_{C-F} = 1.405 Å) > F with another F atom nearby on graphene (E_b = 2.73 eV, l_{C-F} = 1.484 Å) > F on pristine graphene (E_b = −1.92 eV, l_{C-F} = 1.535 Å). Note that the abnormal diffusion barrier of 1.67 eV for diffusion of an F atom at the vacancy along path 3 in Figure 1c is due to the fact that only part of the C−F interaction is broken as discussed above. The actual minimum diffusion barrier is 2.88 eV for diffusion along path 2. In addition, the energy barriers for the F atom diffusing along the different paths at the armchair interface are almost the same ∼2.26 eV, whereas those for the 5 diffusion paths at the zigzag interface are different. The difference in the energy barriers at the zigzag interface are a consequence of the different binding energy of the F−C bond at sites I and II, and the tilt angle between fluorographene and the graphene nanoribbons. The barriers for diffusion from site I along the outside of the angle are always lower than those for diffusions from site II along the inside of the angle. In order to have a more clear idea on the enhanced stability of F atoms on graphene with defects and at the interfaces of GFNRs, the corresponding diffusion times are predicted using eq 2, and they are 4.33×10^9, 4.83×10^{36}, 2.85

DOI: 10.1021/acsami.5b04319
ACS Appl. Mater. Interfaces 2015, 7, 19659−19665

$\times 10^{20}$, and 1.60×10^{26} s for F atoms on graphene with another F atoms, or with a vacancy, and at the zigzag and armchair interfaces of GFNRs, respectively. From the diffusion time, we notice a huge difference of the mobility of F atoms for the different conditions. In addition, it is reported that the electronic and magnetic properties are both interface-orientation- and graphene-width-dependent for the graphene/fluorographene nanoribbons.[36,37] Therefore, electron distribution at the graphene/fluorographene interface is also interface-orientation- and graphene-width-dependent, which would have an important factor for determining the stability of F atoms at the interface. However, the conclusion of the enhanced stability of F atoms at the interface would be expected due to the stronger F−C binding at the interface.

4. CONCLUSION

In conclusion, the diffusion of a single F atom on pristine graphene, graphene with another F atom adsorbed, graphene with a vacancy, and at graphene/fluorographene nanoribbons interfaces are investigated by DFT calculations. It is found that an isolated F atom is able to diffuse easily on a pristine graphene surface with a low energy barrier of about 0.40 eV which results in a predicted diffusion time of 5.78×10^{-6} s. Defects in graphene, such as adsorbates or vacancies, increase the energy barrier significantly, thus preventing the diffusion of F atoms and enhancing the stability of the F atoms on graphene (i.e., the diffusion time increases with at least 10 orders of magnitude). On the other hand, the energy barrier for F atoms at both zigzag and armchair interfaces increases by about a factor 5 as compared to an isolated F on graphene, indicating that F atoms are stable at the graphene/fluorographene interface. The enhancement mechanism is believed to originate from the stronger C−F bonds. Therefore, the stability of F atoms on graphene can be tuned through different techniques, such as inducing defects in graphene and/or creating graphene/fluorographene interfaces, resulting in diffusion times from 10^9 to 10^{36} s. This will localize the F atoms on graphene and therefore will maintain the excellent properties of fluorographene for applications in optoelectronic and photonic nanodevices.

AUTHOR INFORMATION

Corresponding Authors

*E-mail: Zhimin.Ao@uts.edu.au (Z.A.).
*E-mail: Guoxiu.Wang@uts.edu.au (G.W.).

Notes

The authors declare no competing financial interest.

ACKNOWLEDGMENTS

We acknowledge the financial supports from the Chancellor's Research Fellowship Program of the University of Technology Sydney, the Flemish Science Foundation (FWO-Vl) and the Methusalem foundation of the Flemish Government. This research was also supported by the National Computational Infrastructure (NCI) through the merit allocation scheme and used the NCI resources and facilities in Canberra, Australia.

REFERENCES

(1) Tang, Q.; Zhou, Z.; Chen, Z. Graphene-related Nanomaterials: Tuning Properties by Functionalization. *Nanoscale* **2013**, *5*, 4541−4583.

(2) Leenaerts, O.; Peelaers, H.; Hernández-Nieves, A. D.; Partoens, B.; Peeters, F. M. First-principles Investigation of Graphene Fluoride and Graphane. *Phys. Rev. B: Condens. Matter Mater. Phys.* **2010**, *82*, 195436.

(3) Han, S. S.; Yu, T. H.; Merinov, B. V.; van Duin, A. C. T.; Yazami, R.; Goddard, W. A. Unraveling Structural Models of Graphite Fluorides by Density Functional Theory Calculations. *Chem. Mater.* **2010**, *22*, 2142−2154.

(4) Nair, R. R.; Ren, W. C.; Jalil, R.; Riaz, I.; Kravets, V. G.; Britnell, L.; Blake, P.; Schedin, F.; Mayorov, A. S.; Yuan, S. J.; et al. Fluorographene: A Two-Dimenionsional Counterpart of Teflon. *Small* **2010**, *6*, 2877−2884.

(5) Cheng, S. H.; Zou, K.; Okino, F.; Gutierrez, H. R.; Gupta, A.; Shen, N.; Eklund, P. C.; Sofo, J. O.; Zhu, J. Reversible Fluorination of Graphene: Evidence of a Two-dimensional Wide Bandgap Semicondcutor. *Phys. Rev. B: Condens. Matter Mater. Phys.* **2010**, *81*, 205435.

(6) Ho, K. I.; Liao, J. H.; Huang, C. H.; Hsu, C. L.; Zhang, W. J.; Lu, A. Y.; Li, L. J.; Lai, C. S.; Su, C. Y. One-step Formation of a Single Atomic-layer Transistor by the Selective Fluorination of a Graphene Film. *Small* **2014**, *10*, 989−997.

(7) Chen, M.; Zhou, H.; Qiu, C.; Yang, H.; Yu, F.; Sun, L. Layer-dependent Fluorination and Doping of Graphene via Plasma Treatment. *Nanotechnology* **2012**, *23*, 115706.

(8) Zbořil, R.; Karlicky, F.; Bourlinos, A. B.; Steriotis, T. A.; Stubos, A. K.; Georgakilas, V.; Safarova, K.; Jancik, D.; Trapalis, C.; Otyepka, M. Graphene Fluoride: A Stable Stoichiometric Graphene Derivative and its Chemical Conversion to Graphene. *Small* **2010**, *6*, 2885−2891.

(9) Chang, H.; Cheng, J.; Liu, X.; Gao, J.; Li, M.; Li, J.; Tao, X.; Ding, F.; Zheng, Z. Facile Synthesis of Wide-Bandgap Fluorinated Graphene Semiconductors. *Chem. - Eur. J.* **2011**, *17*, 8896−8903.

(10) Tang, S.; Zhang, S. Structural and Electronic Properties of Hybrid Fluorographene-Graphene Nanoribbons: Insight from First-Principles Calculations. *J. Phys. Chem. C* **2011**, *115*, 16644−16651.

(11) Zhu, M.; Xie, X.; Guo, Y.; Chen, P.; Ou, X.; Yu, G.; Liu, M. Fluorographene Nanosheets with Broad Solvent Dispersibility and Their Applications as a Modified Layer in Organic Field-effect Transistors. *Phys. Chem. Chem. Phys.* **2013**, *15*, 20992−21000.

(12) Jeon, K.; Lee, Z.; Pollak, E.; Moreschini, L.; Bostwick, A.; Park, C.; Mendelsberg, R.; Radmilovic, V.; Kostecki, R.; Richardson, T.; et al. Fluorographene: A Wide Bandgap Semicondutor with Ultraviolet Luminescence. *ACS Nano* **2011**, *5*, 1042−1046.

(13) Charlier, J. C.; Gonze, X.; Michenaud, J. P. First-principles Study of Graphite Monofluoride $(CF)_n$. *Phys. Rev. B: Condens. Matter Mater. Phys.* **1993**, *47*, 16162.

(14) Robinson, J. T.; Burgess, J. S.; Junkermeier, C. E.; Badescu, S. C.; Reinecke, T. L.; Perkins, F. K.; Zalalutdniov, M. K.; Baldwin, J. W.; Culbertson, J. C.; Sheehan, P. E.; et al. Properties of Fluorinated Graphene Films. *Nano Lett.* **2010**, *10*, 3001−3005.

(15) Liu, H. Y.; Hou, Z. F.; Hu, C. H.; Yang, Y.; Zhu, Z. Z. Electronic and Magnetic Properties of Fluorinated Graphene with Different Coverage of Fluorine. *J. Phys. Chem. C* **2012**, *116*, 18193−18201.

(16) Withers, F.; Bointon, T. H.; Dubois, M.; Russo, S.; Craciun, M. F. Nanopatterning of Fluorinated Graphene by Electron Beam Irradiation. *Nano Lett.* **2011**, *11*, 3912−3916.

(17) Lee, W. H.; Suk, J. W.; Chou, H.; Lee, J. H.; Hao, Y.; Wu, Y. F.; Piner, R.; Akinwande, D.; Kim, K. S.; Ruoff, R. S. Selective-Area Fluorination of Graphene with Fluoropolymer and Laser Irradiation. *Nano Lett.* **2012**, *12*, 2374−2378.

(18) Moon, J. S.; Seo, H. C.; Stratan, F.; Antcliffe, M.; Schmitz, A.; Ross, R. S.; Kiselev, A. A.; Wheeler, V. D.; Nyakiti, L. O.; Gaskill, D. K.; et al. Lateral Graphene Heterostructure Field-Effect Transistor. *IEEE Electron Device Lett.* **2013**, *34*, 1190−1192.

(19) Tozzini, V.; Pellegrini, V. Electronic Stucture and Peierls Instability in Graphene Nanoribbons Sculpted in Graphane. *Phys. Rev. B: Condens. Matter Mater. Phys.* **2010**, *81*, 113404.

(20) Ao, Z. M.; Hernández-Nieves, A. D.; Peeters, F. M.; Li, S. Enhanced Stability of Hydrogen Atoms at the Graphene/graphane Interface of Nanoribbons. *Appl. Phys. Lett.* **2010**, *97*, 233109.

DOI: 10.1021/acsami.5b04319
ACS Appl. Mater. Interfaces 2015, 7, 19659−19665

(21) Santos, H.; Henrard, L. Fluorine Adsorption on Single and Bilayer Graphene: Role of Sublattice and Layer Decoupling. *J. Phys. Chem. C* **2014**, *118*, 27074−27080.
(22) Medeiros, P. V. C.; Mascarenhas, A. J. S.; de Brito Mota, F.; de Castilho, C. M. C. A DFT Study of Halogen Atoms Adsorbed on Graphene Layers. *Nanotechnology* **2010**, *21*, 485701.
(23) Wu, B. R.; Yang, C. K. Electronic Structures of Graphene with Vacancies and Graphene Adsorbed with Fluorine Atoms. *AIP Adv.* **2012**, *2*, 012173.
(24) Sofo, J. O.; Suarez, A. M.; Usaj, G.; Cornaglia, P. S.; Hernandez-Nieves, A. D.; Balseiro, C. A. Electrical Control of the Chemical Bonding of Fluorine on Graphene. *Phys. Rev. B: Condens. Matter Mater. Phys.* **2011**, *83*, 081411.
(25) Kim, H. J.; Cho, J. H. Fluorine-induced Local Magnetic Moment in Graphene: A Hybrid DFT Study. *Phys. Rev. B: Condens. Matter Mater. Phys.* **2013**, *87*, 174435.
(26) Young, D. C. *Computational Chemistry: A Practical Guide for Applying Techniques to Real World Problems*; John Wiley & Sons, Inc.: Hoboken, NJ, 2002.
(27) Jiang, Q. G.; Ao, Z. M.; Li, S.; Wen, Z. Density Functional Theory Calculations on the CO Catalytic Oxidation on Al-embeded Graphene. *RSC Adv.* **2014**, *4*, 20290−20296.
(28) Krasheninnikov, A. V.; Lehtinen, P. O.; Foster, A. S.; Pyykkö, P.; Nieminen, R. M. Embedding Transition-Metal Atoms in Graphene: Structure, Bonding, and Magnetism. *Phys. Rev. Lett.* **2009**, *102*, 126807.
(29) Pauling, L. C. *General Chemistry*; Dover Publications: New York, 1988.
(30) Kittel, C. *Introduction to Solid State Physics*; John Wiley & Sons, Inc.: Hoboken, NJ, 1996.
(31) Holz, M.; Heil, S. R.; Sacco, A. Temperature-dependent Self-diffusion Coefficients of Water and Six Selected Molecular Liquids for Calibration in Accurate ^{1}H NMR PFG Measurements. *Phys. Chem. Chem. Phys.* **2000**, *2*, 4740−4742.
(32) Ao, Z. M.; Hernández-Nieves, A. D.; Peeters, F. M.; Li, S. The Electric Field as a Novel Switch for Uptake/release of Hydrogen for Storage in Nitrogen Doped Graphene. *Phys. Chem. Chem. Phys.* **2012**, *14*, 1463−1467.
(33) Hirshfeld, F. L. Bonded-atom Fragments for Describing Molecular Charge Densities. *Theor. Chim. Acta* **1977**, *44*, 129−138.
(34) Boukhvalov, D. W. Modeling of Hydrogen and Hydroxyl Group Migration on Graphene. *Phys. Chem. Chem. Phys.* **2010**, *12*, 15367−15371.
(35) Grimme, S. Semiempirical GGA-type Density Functional Constructed with a Long-range Dispersion Correction. *J. Comput. Chem.* **2006**, *27*, 1787−1799.
(36) Shi, H.; Pan, H.; Zhang, Y.-W.; Yakobson, B. I. Electronic and Magnetic Properties of Graphene/Fluorographene Superlattices. *J. Phys. Chem. C* **2012**, *116*, 18278−18283.
(37) Tang, S.; Cao, X. Realizing Semiconductor-half-metal Transition in Zigzag Graphene Nanoribbons Supported on Hybrid Fluorographene-graphane Nanoribbons. *Phys. Chem. Chem. Phys.* **2014**, *16*, 23214−23223.

DOI: 10.1021/acsami.5b04319
ACS Appl. Mater. Interfaces 2015, 7, 19659−19665